

# MS spectra of the identified compounds

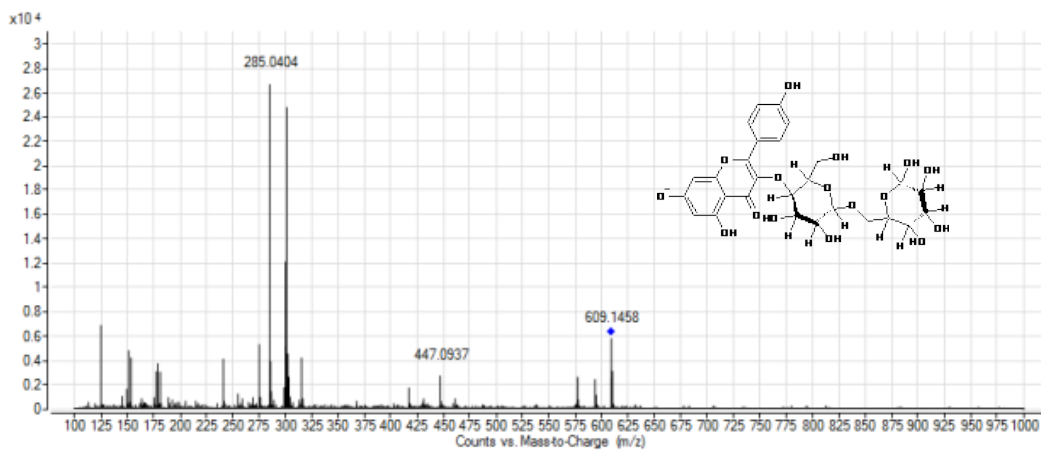


Fig. S1. Mass spectrum of kaempferol -O-dihexoside (peak 1)

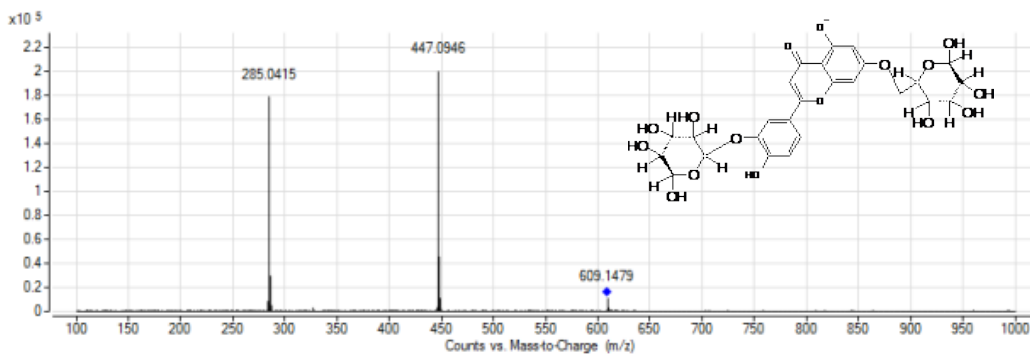


Fig. S2. Mass spectrum of luteolin 3', 7'-O-diglucoside (peak 2)

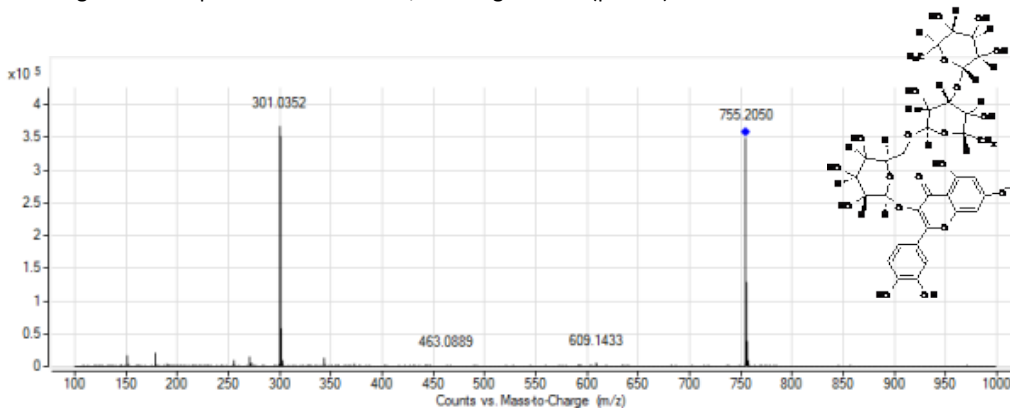


Fig. S3. Mass spectrum of quercetin -O-dirhamnoside glucoside (peak 3)

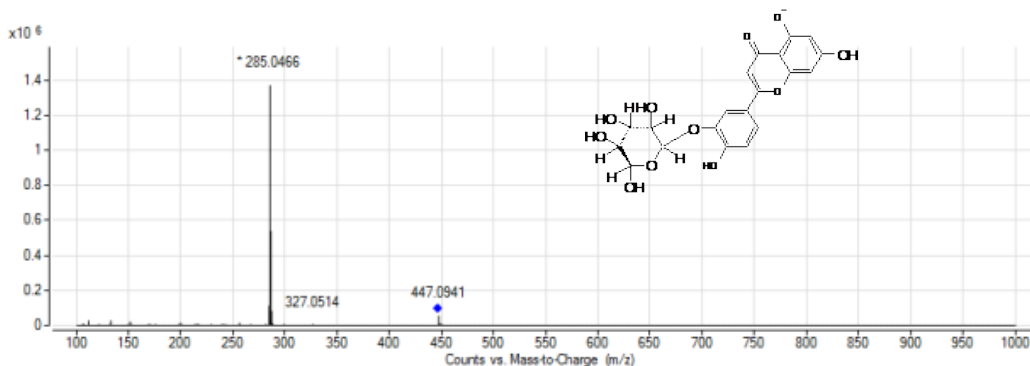


Fig. S4. Mass spectrum of luteolin -O-glucoside (peak 4)

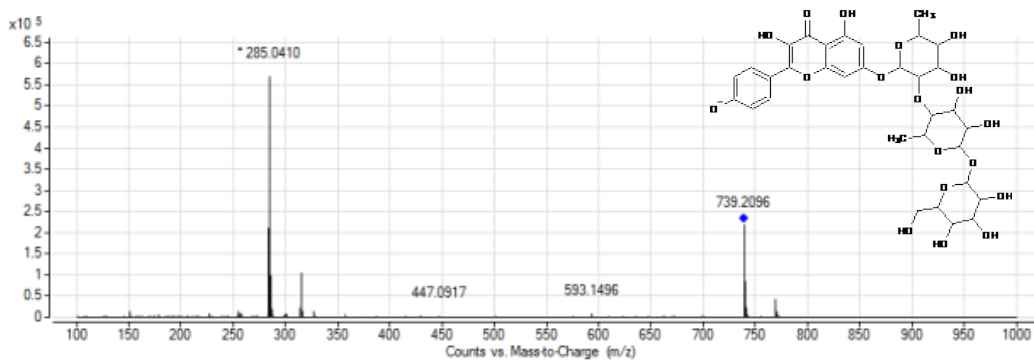


Fig. S5. Mass spectrum of kaempferol-O-dirhamnoside-glucoside (peak 5)

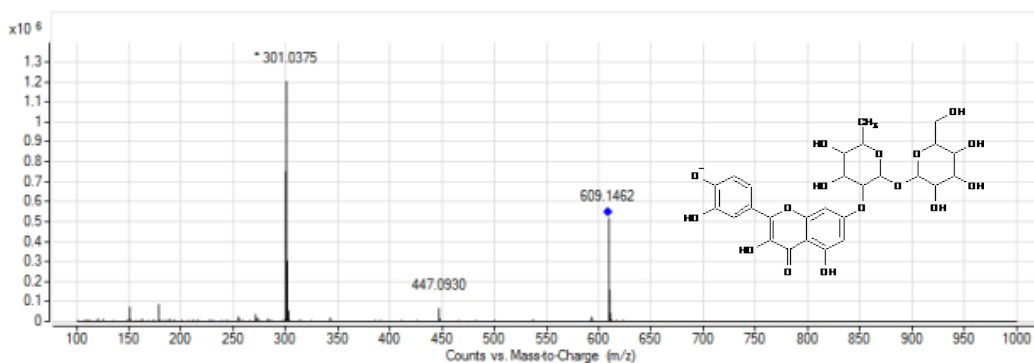


Fig. S6. Mass spectrum of quercetin-O-rhamnoside-glucoside (peak 6)

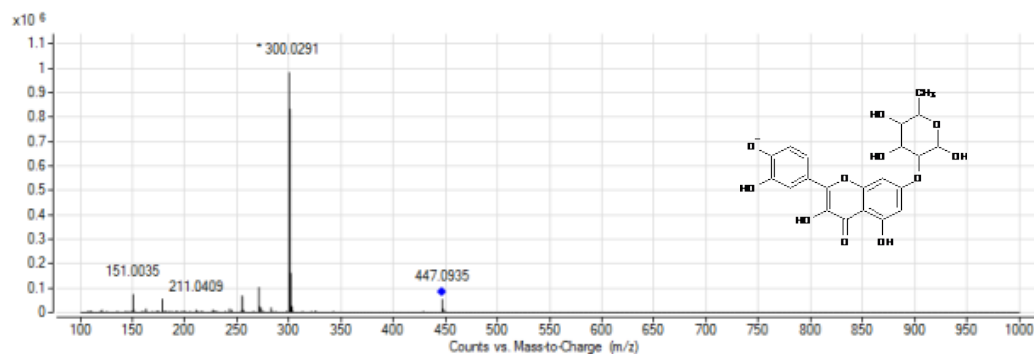


Fig. S7. Mass spectrum of quercetin-O-rhamnoside (peak 7)

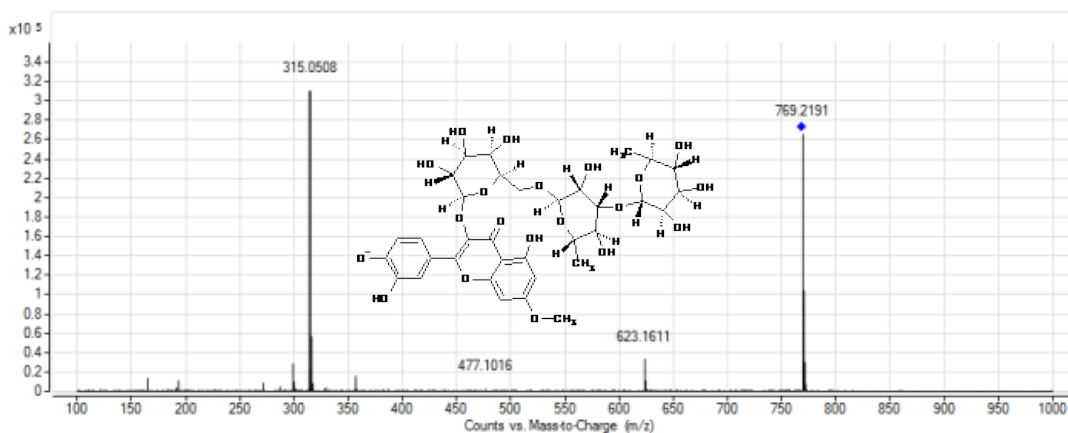


Fig. S8. Mass spectrum of rhamnetin-O-dirhamnoside-glucoside (peak 8)

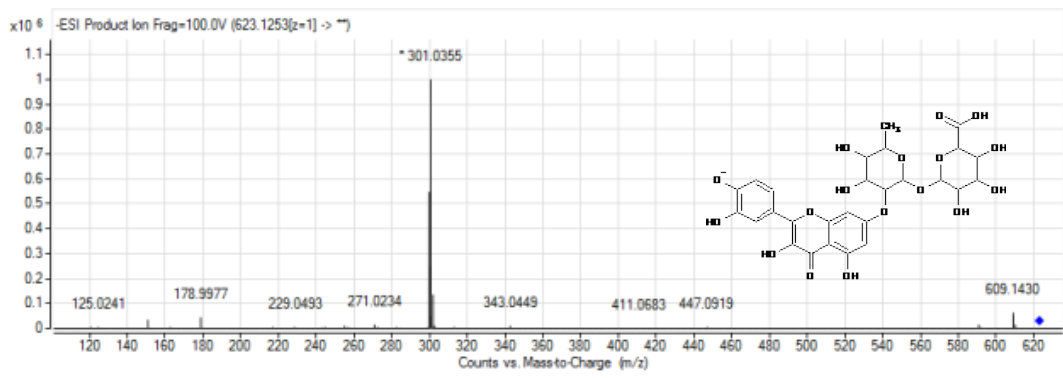


Fig. S9. Mass spectrum of quercetin-*O*-rhamnoside –glucuronide (peak 9)

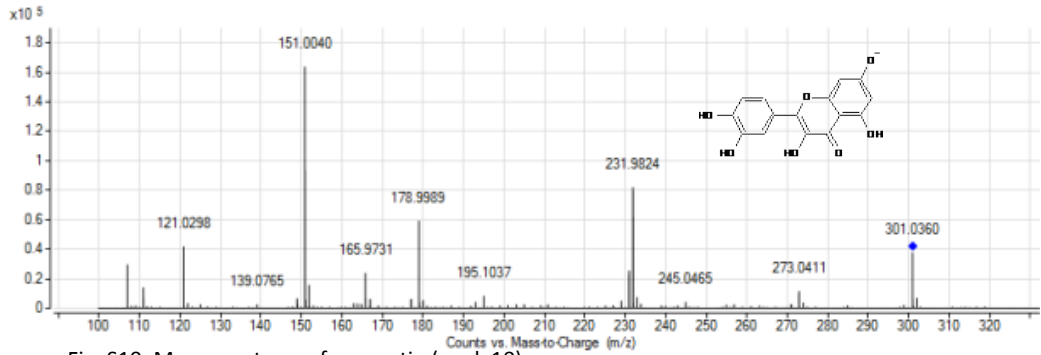


Fig. S10. Mass spectrum of quercetin (peak 10)

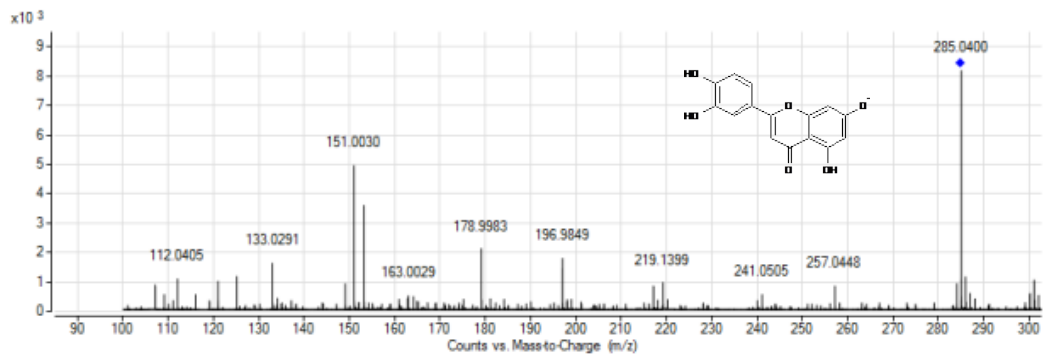


Fig. S11. Mass spectrum of luteolin (peak 11)

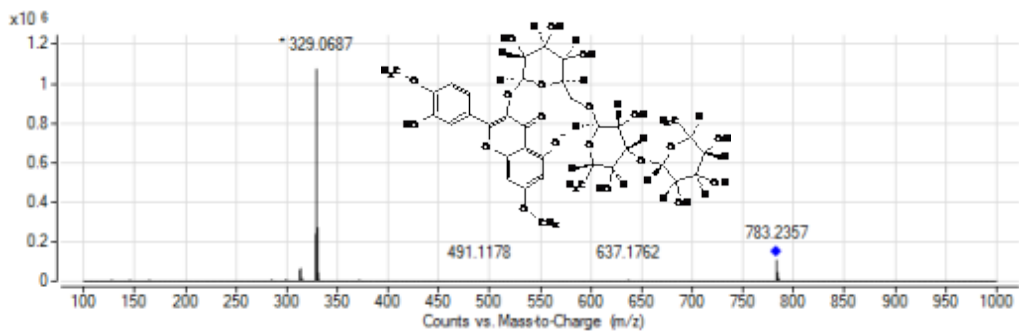


Fig. S12. Mass spectrum of rhamnazin-3-*O*-rhamnoside (peak 12)

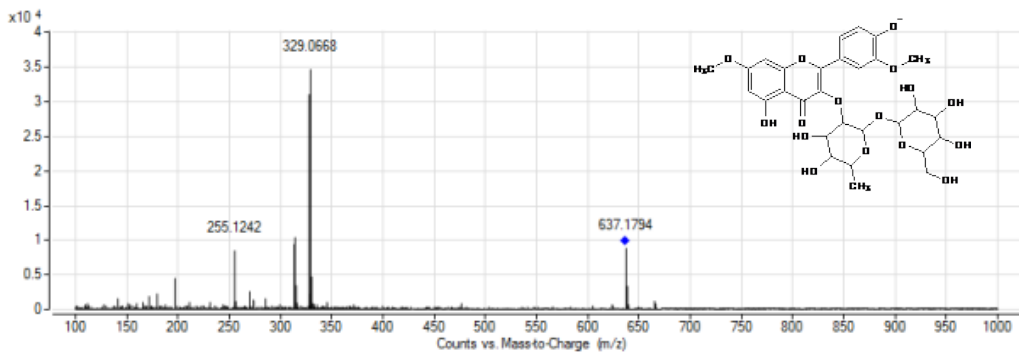


Fig. S13 Mass spectrum of rhamnazin-O-rhamnoside-glycoside (peak 13)

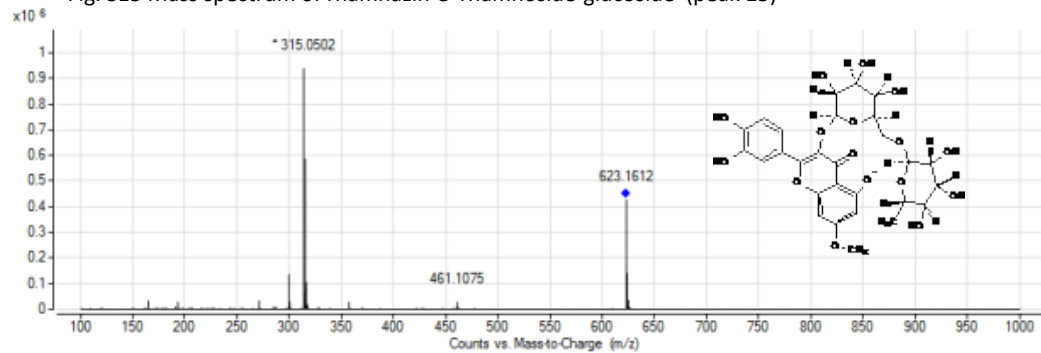


Fig. S14. Mass spectrum of rhamnetin-3-O-rhamnoside (peak 14)

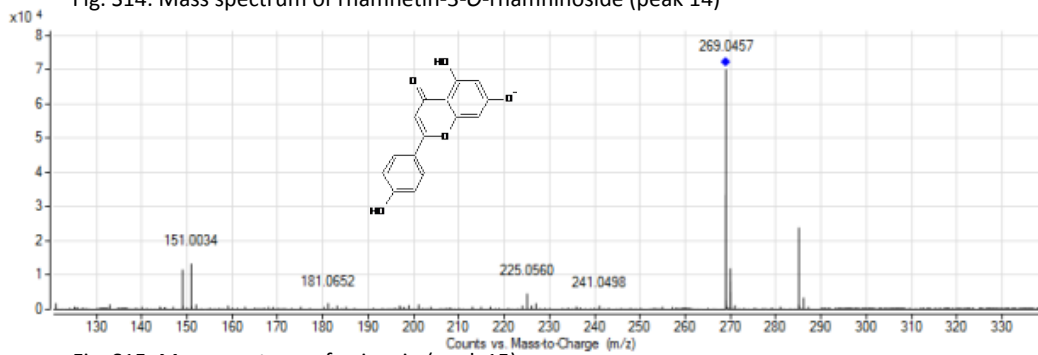


Fig. S15. Mass spectrum of apigenin (peak 15)

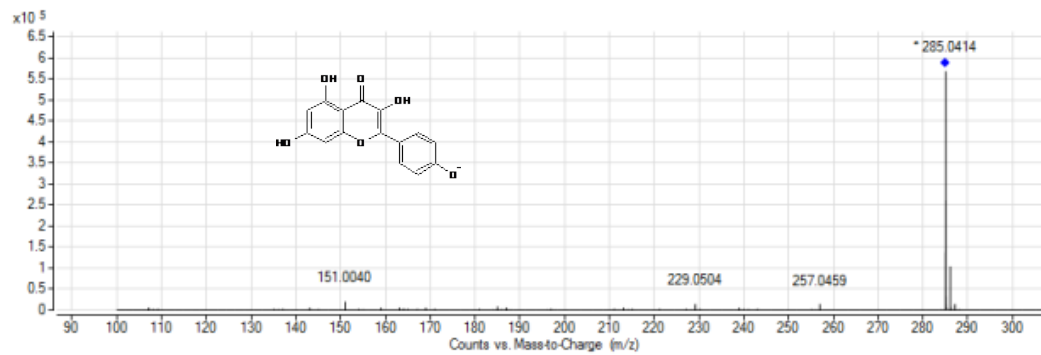
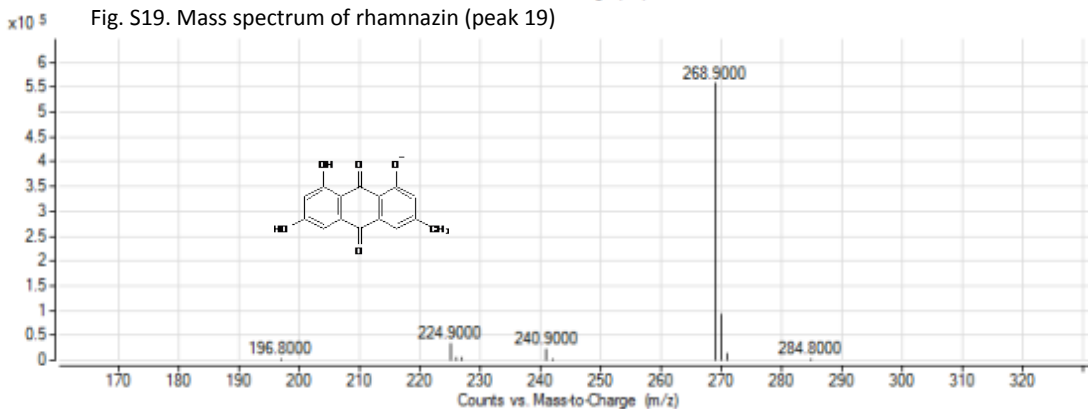
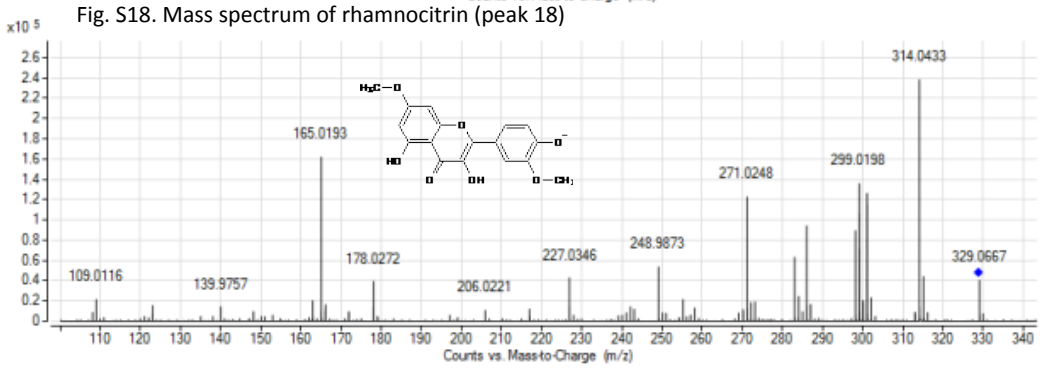
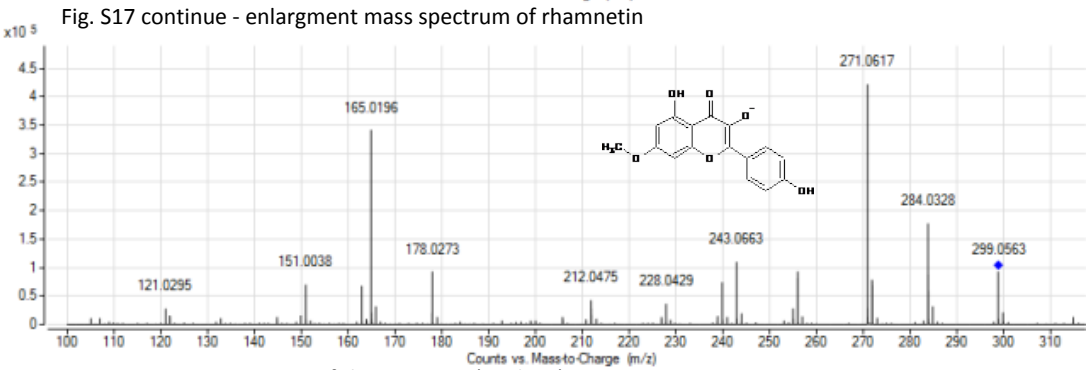
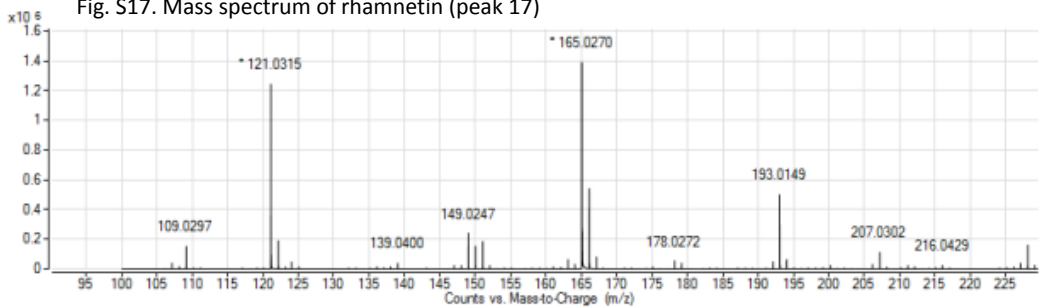
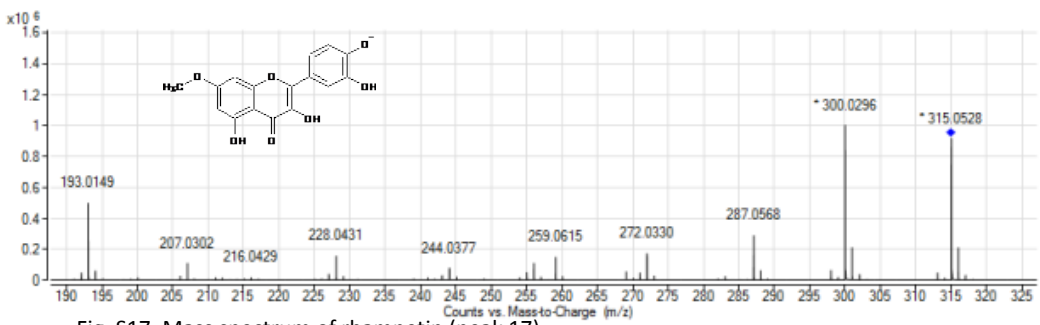


Fig. S16. Mass spectrum of kaempferol (peak 16)



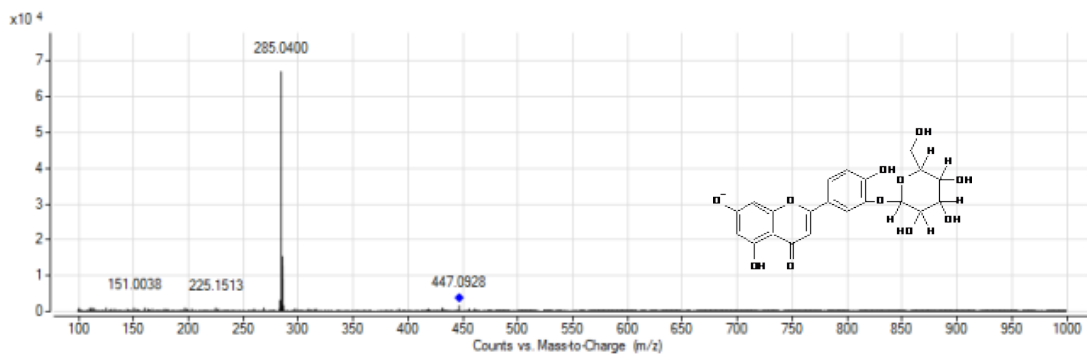


Fig. S21. Mass spectrum of luteolin-O-glucoside (peak 21)

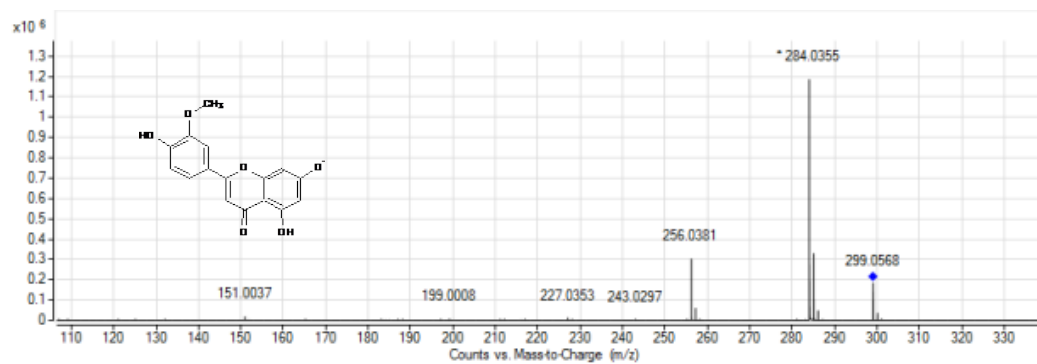


Fig. S22. Mass spectrum of chrysoeriol (peak 22)

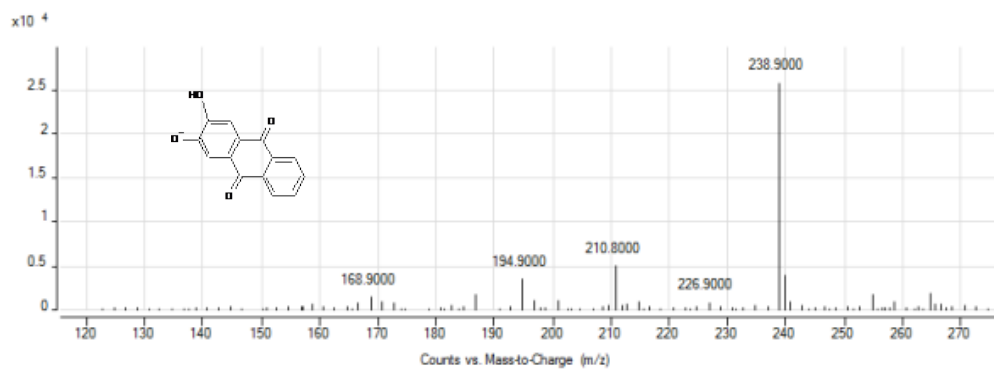


Fig. S23. Mass spectrum of hystazarin (peak 23)

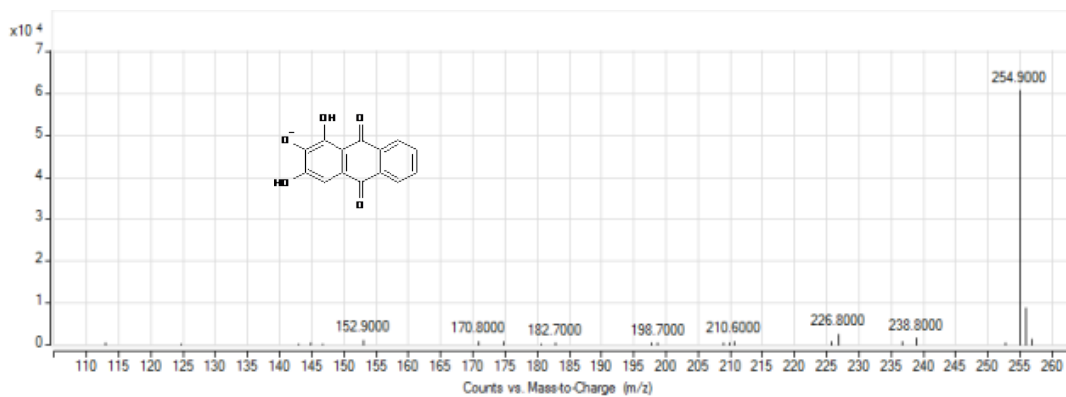


Fig. S24. Mass spectrum of anthragallol (peak 24)

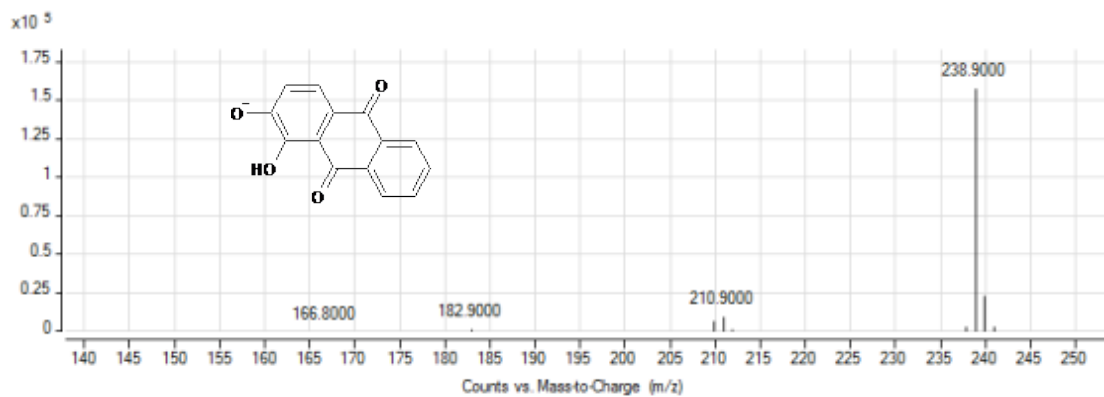


Fig. S25. Mass spectrum of alizarin (peak 25)

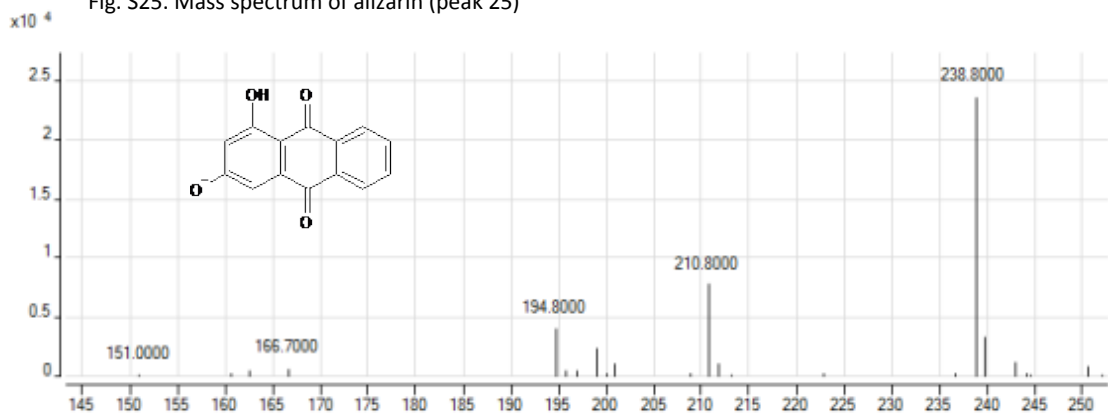


Fig. S26. Mass spectrum of xanthopurpurin (peak 26)

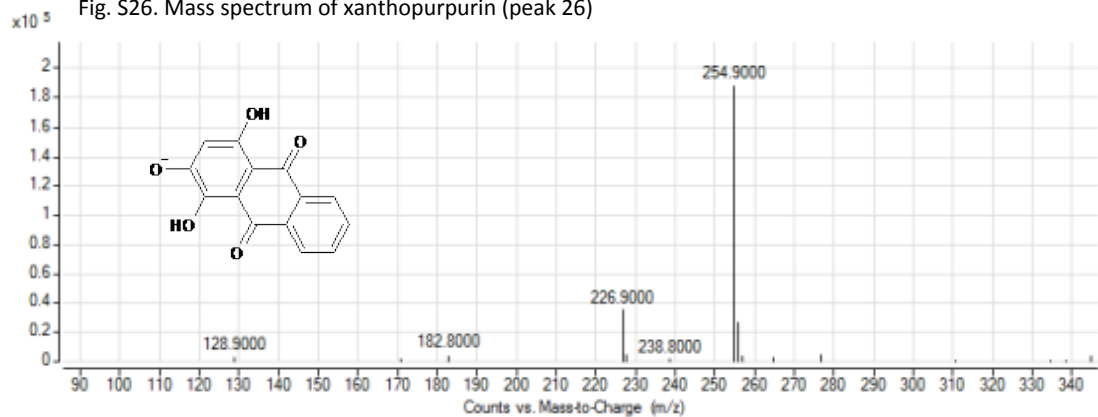


Fig. S27. Mass spectrum of purpurin (peak 27)

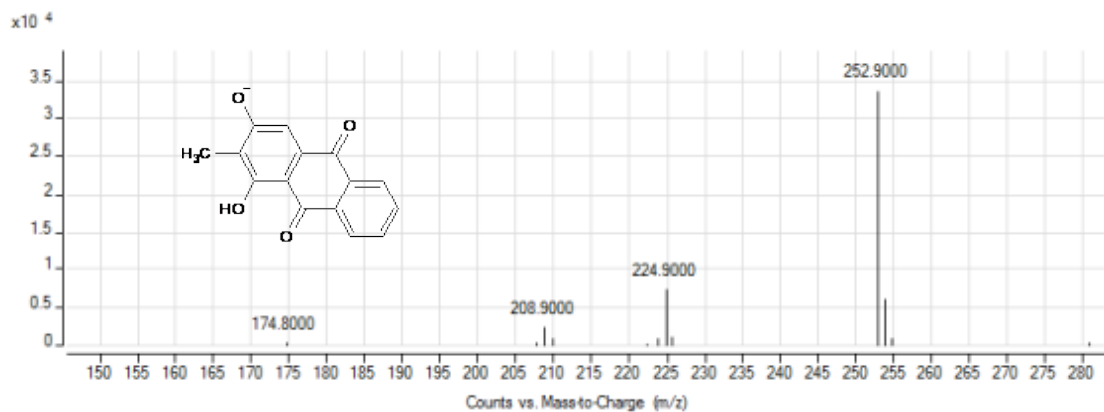


Fig. S28. Mass spectrum of rubiadin (peak 28)

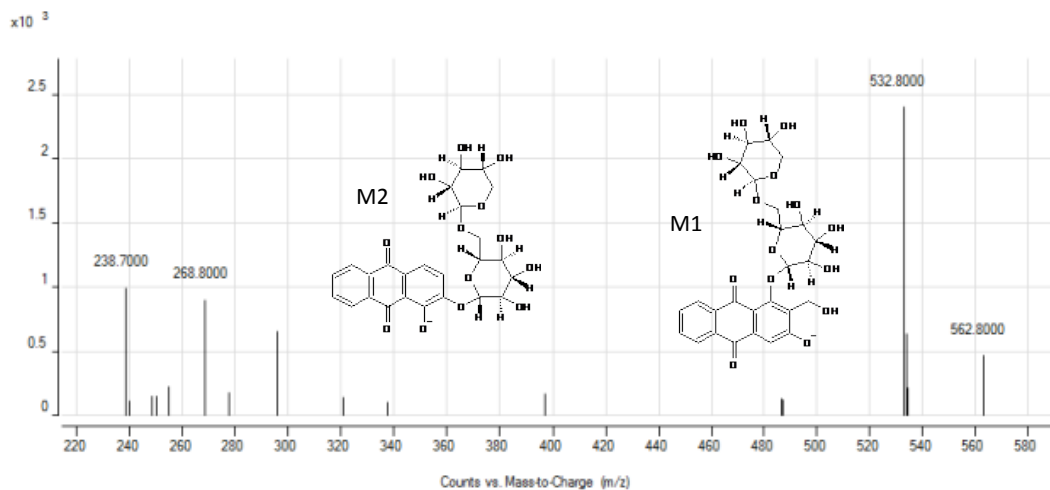


Fig. S29. Mass spectrum of lucidin primeveroside and alizarin primeveroside (peak M1 and M2)

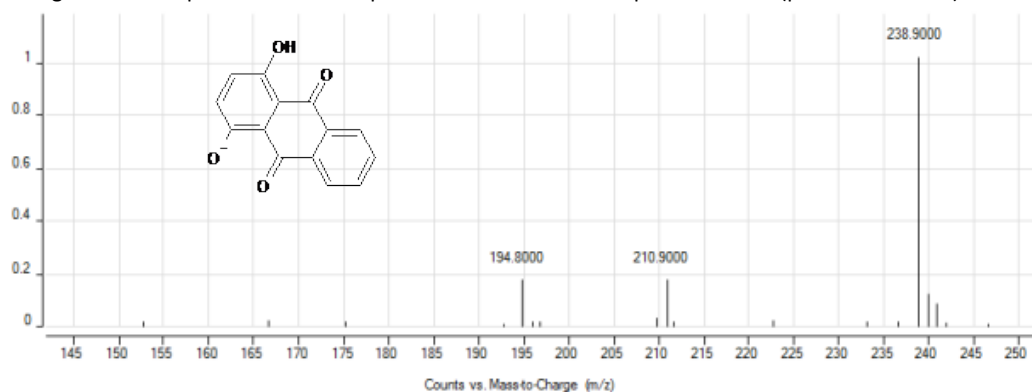


Fig. S30. Mass spectrum of Quinizarin (peak M3)

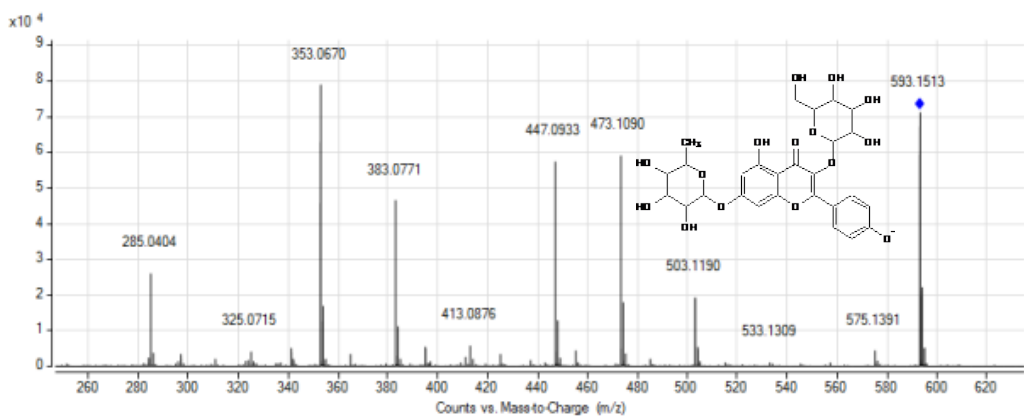


Fig. S31. Mass spectrum of kaempferol-O-glucoside-O-rhamnoside (peak W1)

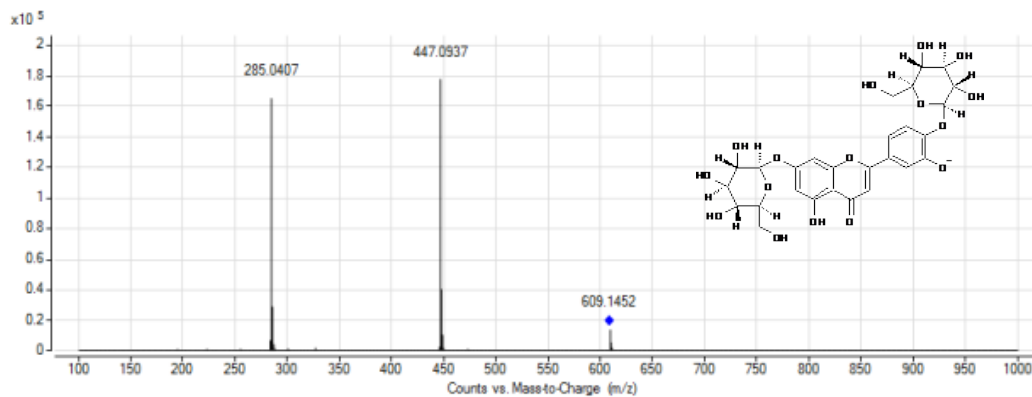


Fig. S32. Mass spectrum of luteolin-O-diglucoside (peak W2)



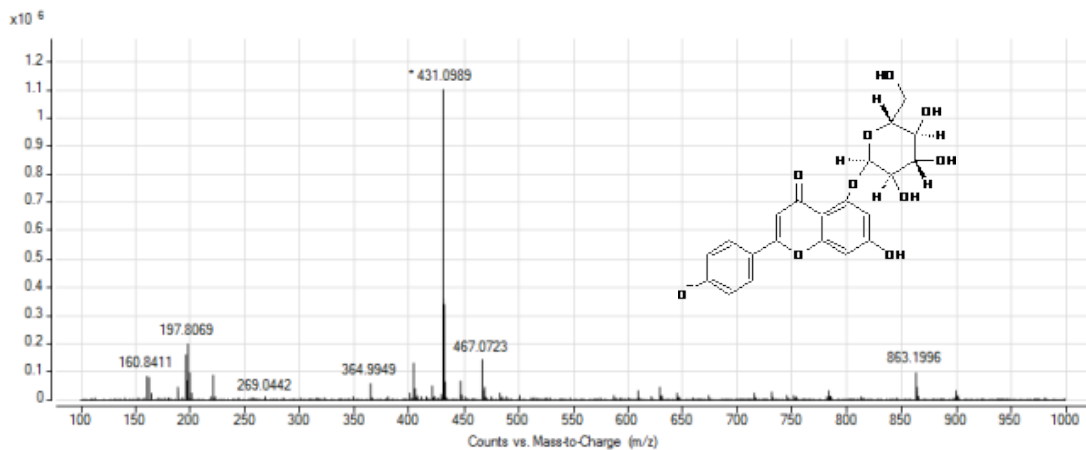


Fig. S33. Mass spectrum of apigenin-O-glucoside (peak W3)

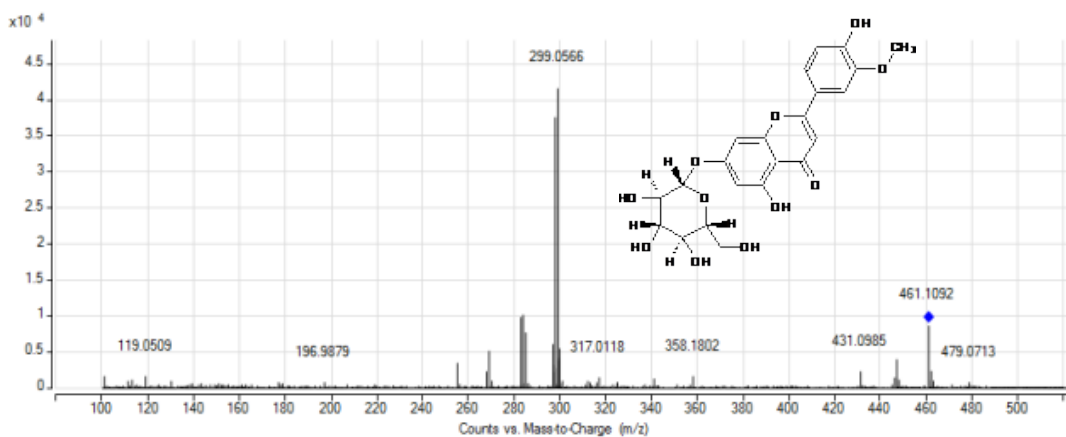


Fig. S34. Mass spectrum of chrysoeriol-O-glucoside (peak W4)

## Laque de Robert No. 5 paint sample

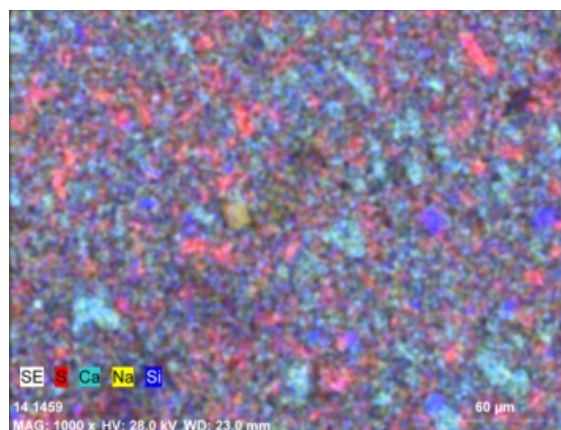
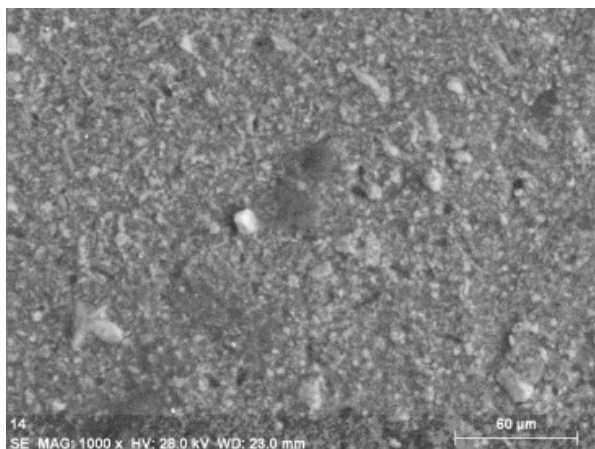
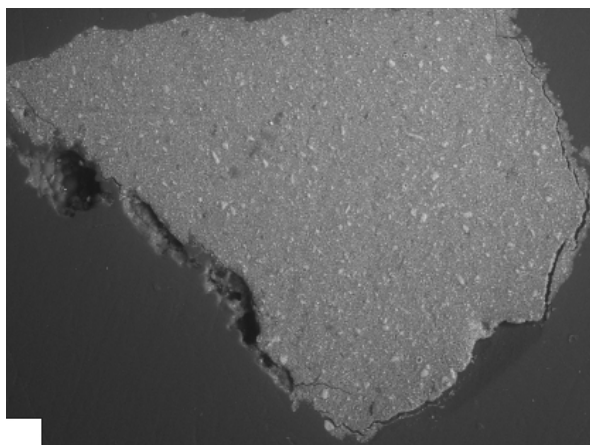


Fig. S35. Microscopic (200x) and BSE images and SEM-EDX map of elemental distribution (1000 x) of the *Laque de Robert No. 5* paint sample. Elements identified using SEM-EDX: Ca, Al, S, K, Si, Mg, Na and Fe, Zn . All these elements apart from Na were confirmed with the XRF analyses, moreover Sn was detected as well. BSE image reveals grains of zinc white embedded within the lake matrix. SEM-EDX map of elemental distribution (1000 x) showing grain of chalk and silica sand within the matrix of lake precipitated on aluminum and tin compounds. Sn was detected

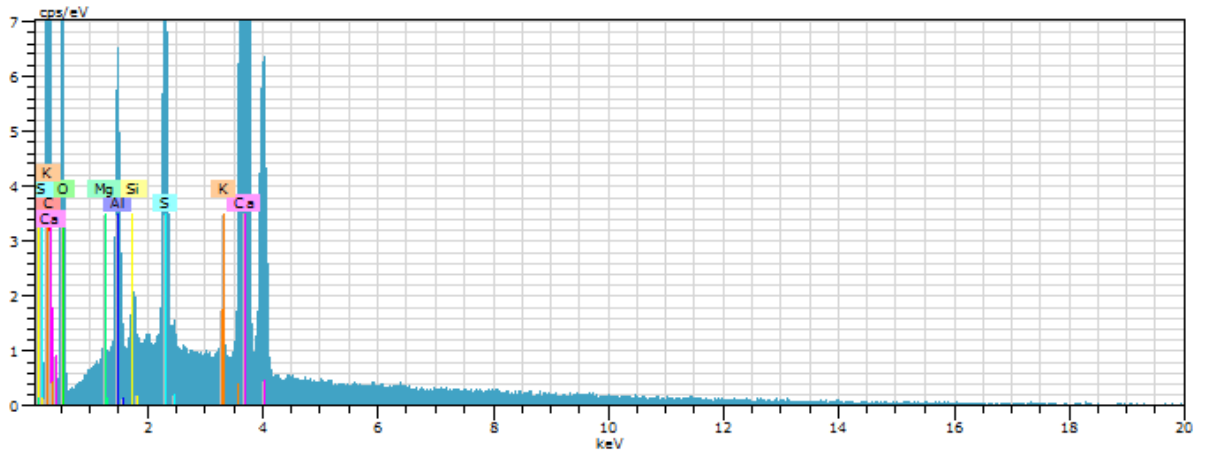
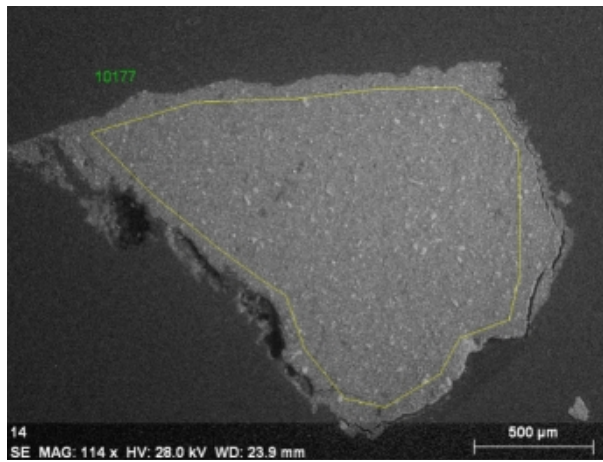


Fig. S36a. SEM-EDX spectrum of of the *Laque de Robert No. 5* paint sample.

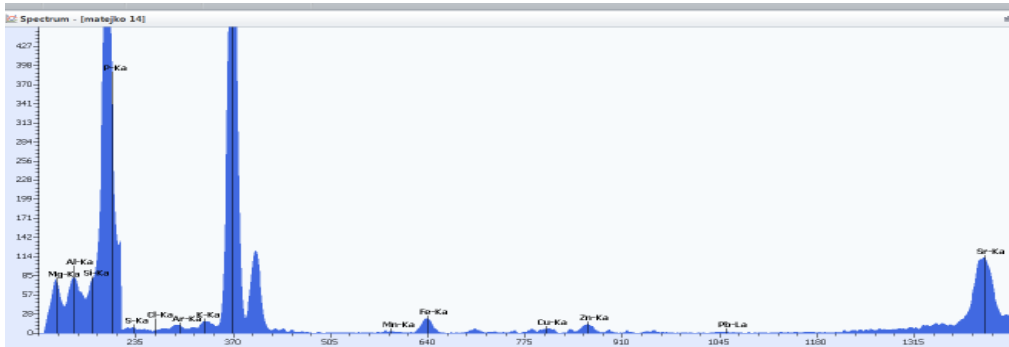
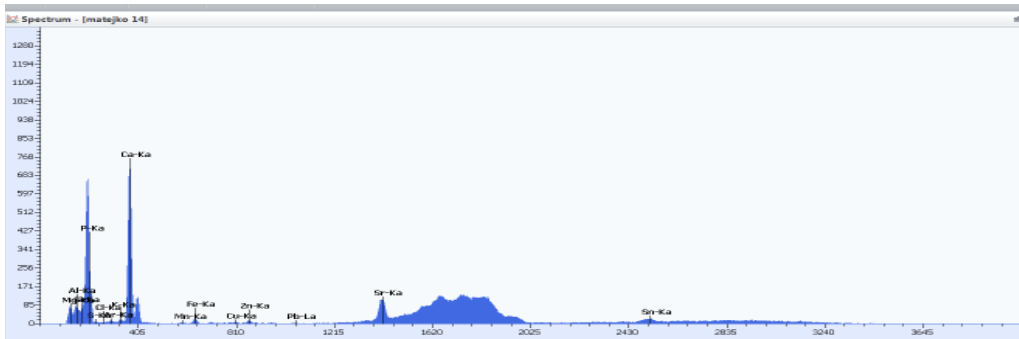


Fig. S36b. XRF spectra of the *Laque de Robert No. 5* paint sample.

## *Laque de Robert No. 6* paint sample

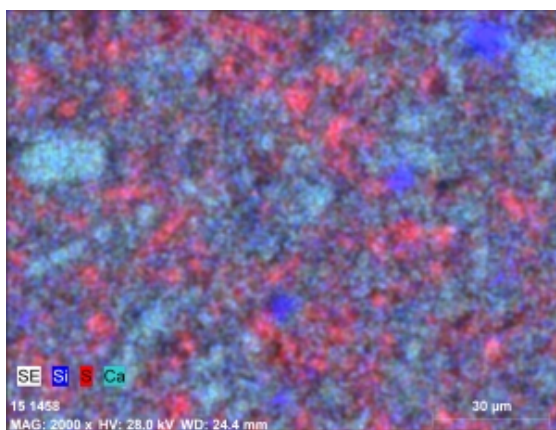
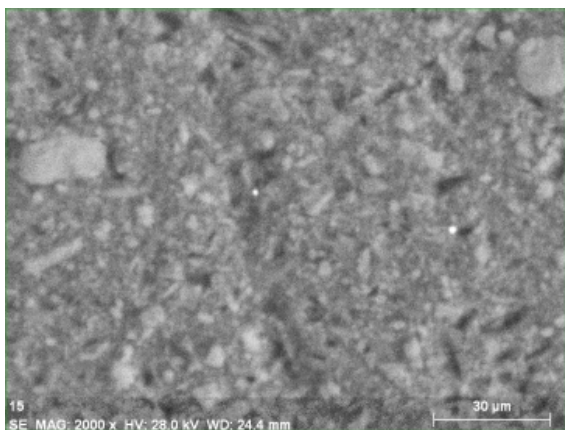
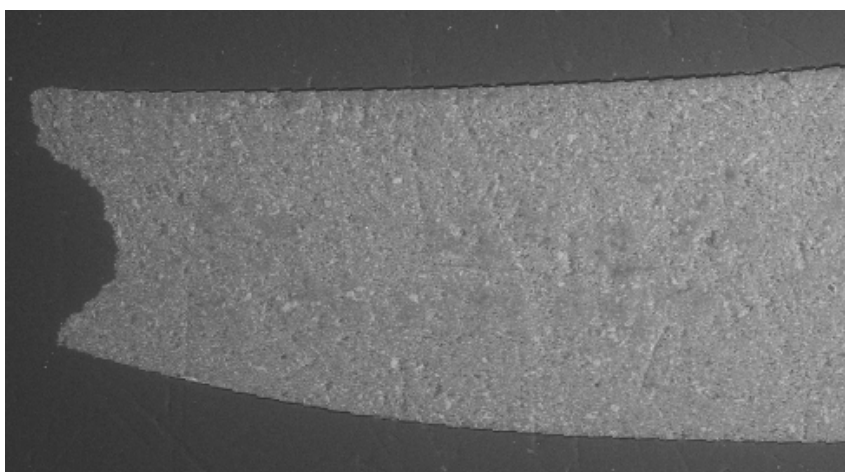


Fig. S37. Microscopic (200x) and BSE images and SEM-EDX map of elemental distribution (1000 x) of the *Laque de Robert No. 6* paint sample. Elements identified using SEM-EDX: Ca, S, Al., K, Si, Mg. Zinc white not present. All these elements were confirmed with the XRF analyses, moreover Sn was detected as well. SEM-EDX map of elemental distribution showing grains of chalk and silica sand within the matrix of lake precipitated on aluminum and tin compounds.

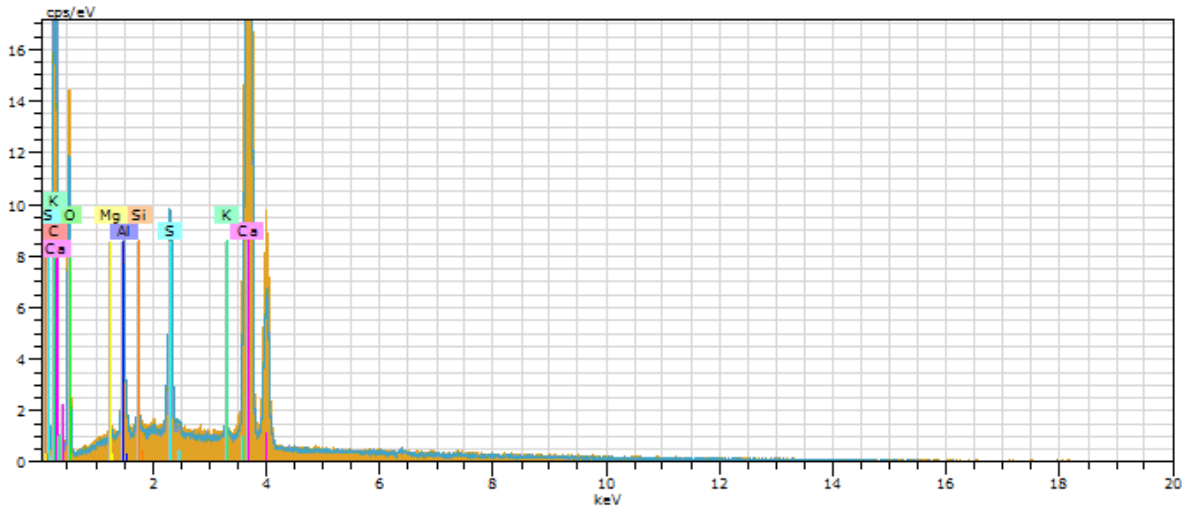
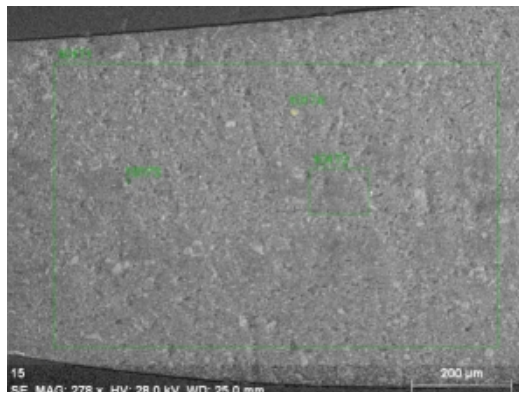


Fig. S38a. SEM-EDX spectrum of of the *Laque de Robert No. 6* paint sample.



Fig. S38b. XRF spectrum of the *Laque de Robert No. 6* paint sample compared with the *Laque de Robert No. 5* spectrum (yellow line). Lesser amount of Ca, P and Sr were detected.



## *Still de Grain* paint sample

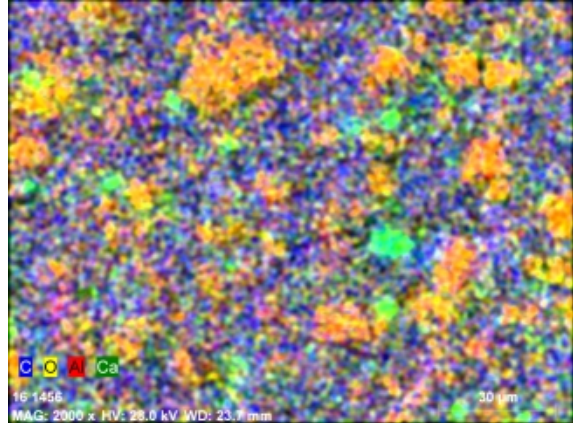
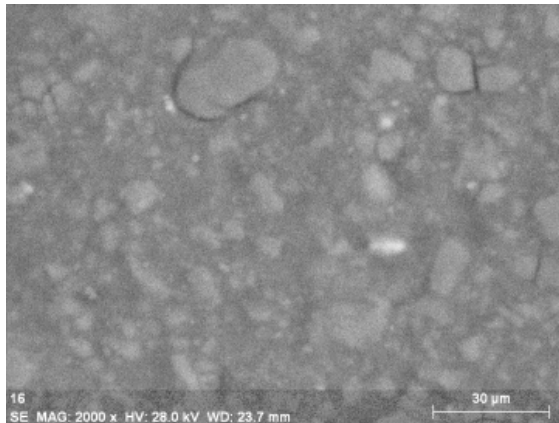
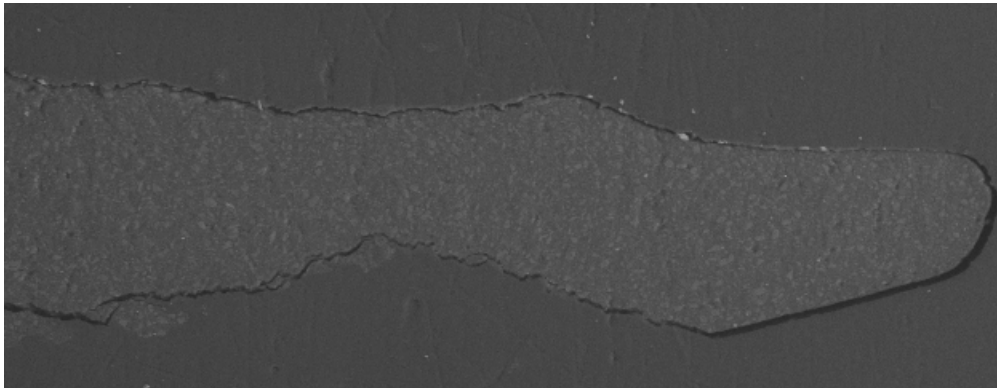
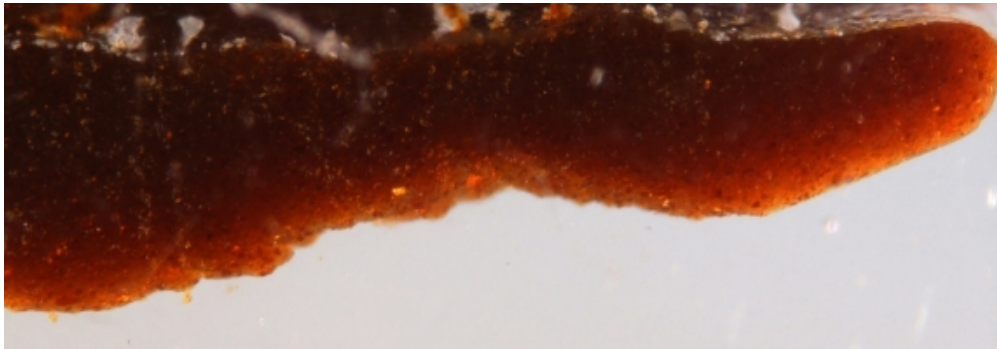


Fig. S39. Microscopic (200x) and BSE images and SEM-EDX map of elemental distribution (1000 x) of the *Still de Grain* paint sample, Elements identified using SEM-EDX : Al, Ca, Si, K, Cl, S, P, Mg, Na. All these elements apart from Na were confirmed with the XRF analyses. Phosphorus probably of plant origin. Homogenous texture of the finely ground paint visible. SEM-EDX map of elemental distribution showing grains of chalk within the matrix of lake precipitated on aluminum compounds.

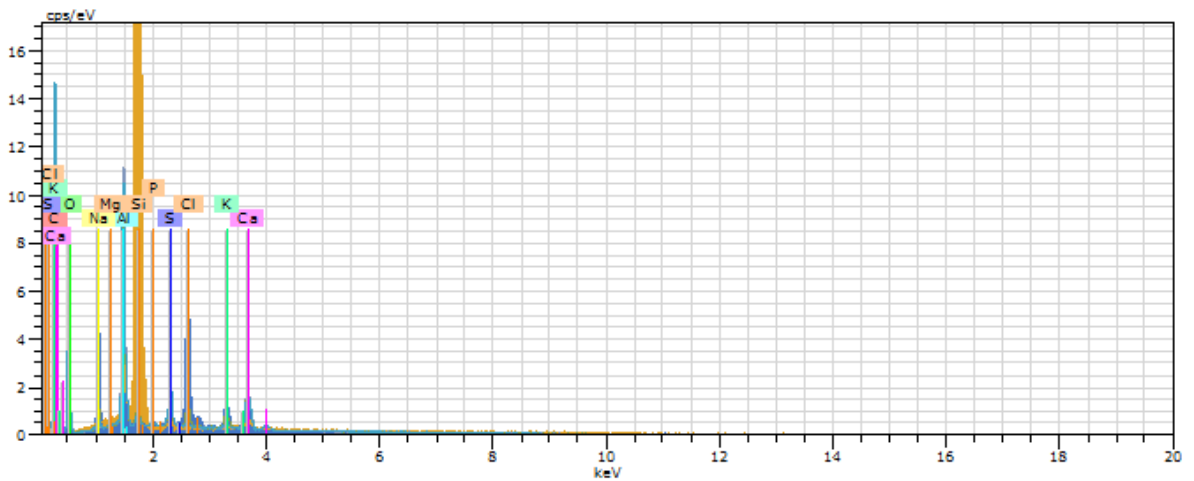
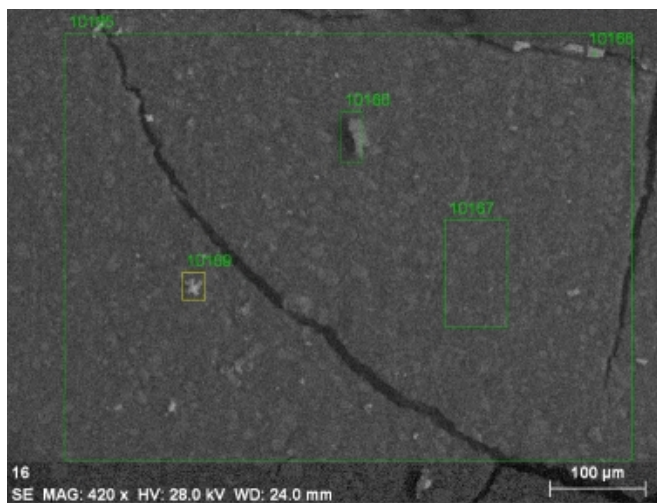


Fig. S40a. SEM-EDX spectra of the *Still de Grain* paint sample.

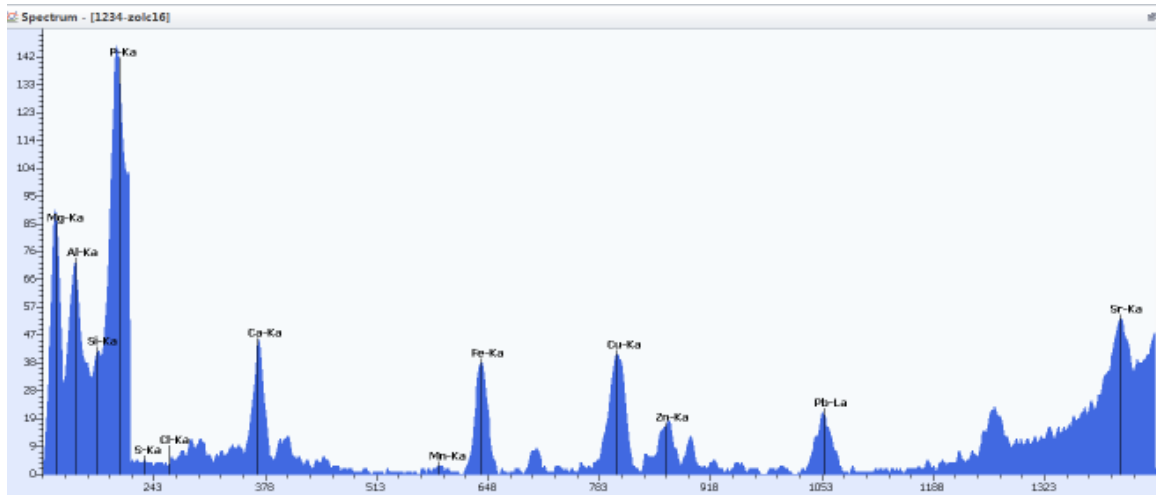


Fig. S40b. XRF spectrum of the *Still de Grain* paint sample. Elements identified: P, Ca, Fe, Cu, Pb, Zn, Sr, Mg, Al, Si, S, Mn and K.

## *Laque de Garance* paint sample

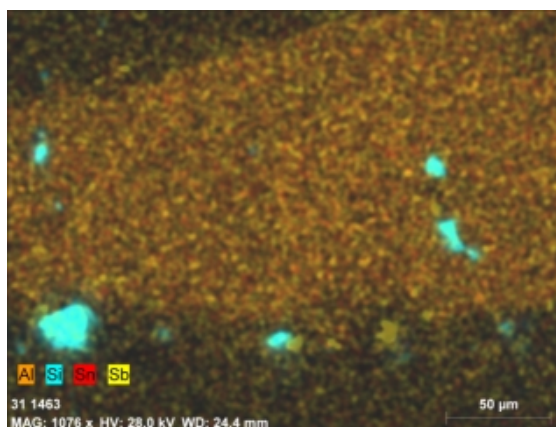
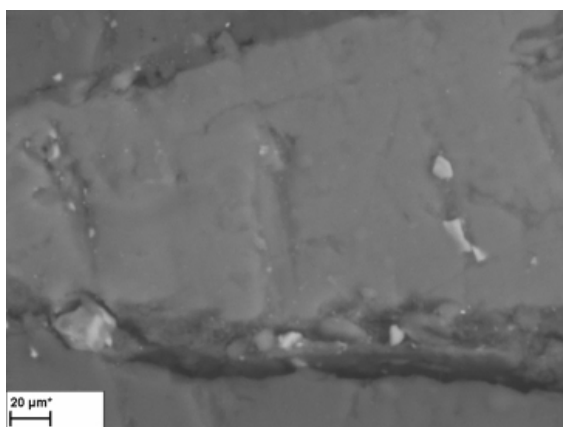
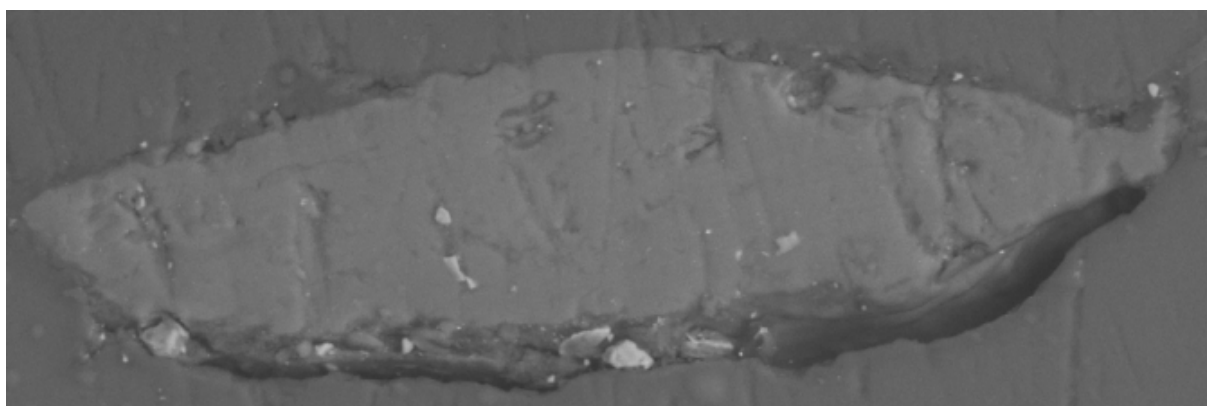
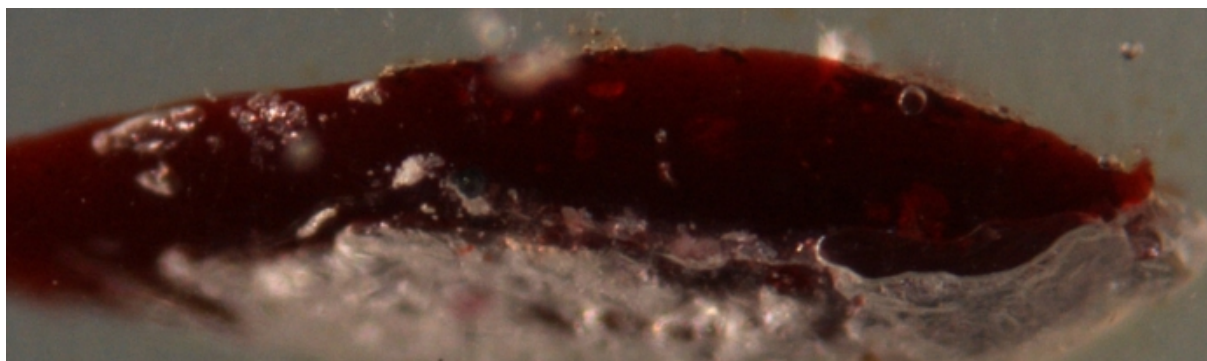


Fig. S41. Microscopic (200x) and BSE images and SEM-EDX map of elemental distribution (1000 x) of the *Laque de Garance* paint sample. Elements identified using SEM-EDX Al, P, Sn, Si, Ca, S and Sb. All these elements were confirmed with the XRF analyses, moreover Sn and Pb were detected as well. The lake precipitated on amorphous aluminum hydrate, tin salts and chalk. Phosphorus of plant origin. Homogeneously distributed within all the paint, only grains of silica sand visible as distinguishable grains.



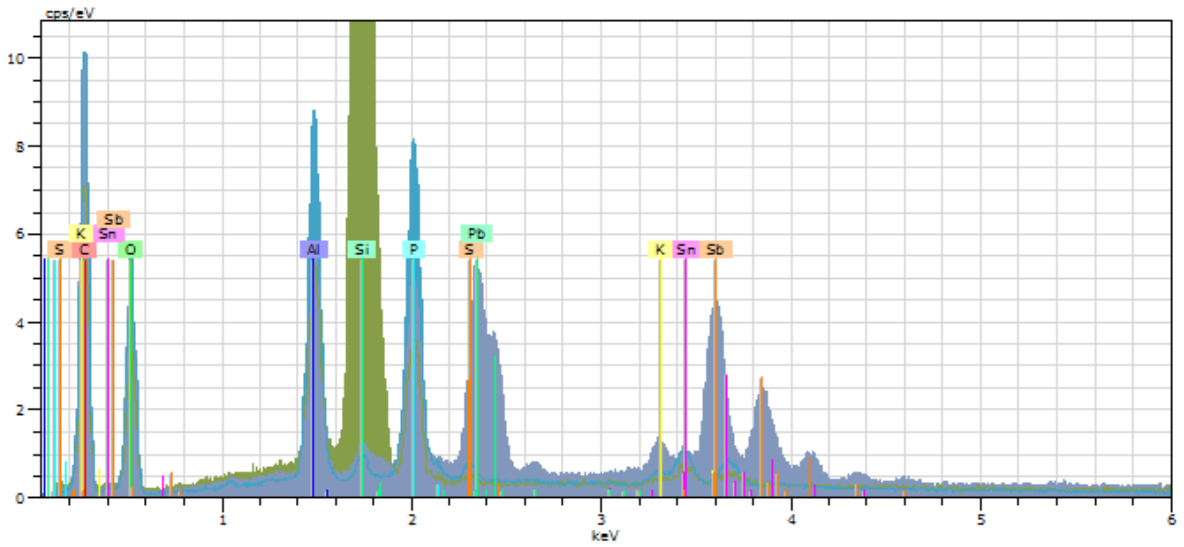
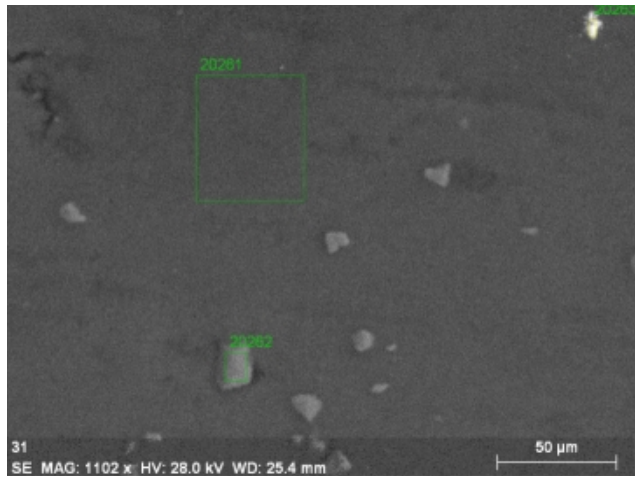


Fig. S42a. SEM-EDX spectra of the *Laque de Garance* paint sample.

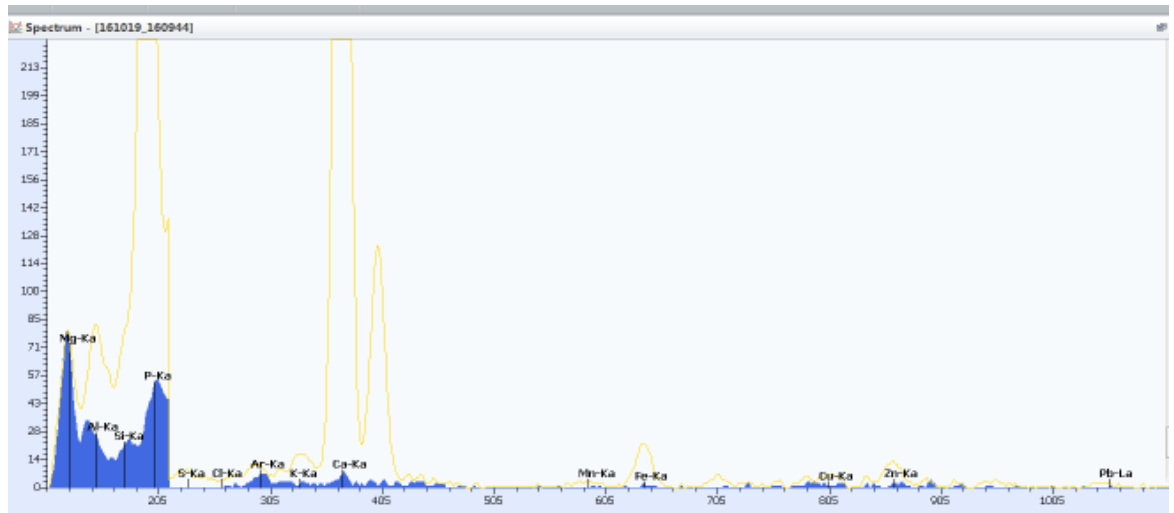


Fig. S42b. XRF spectrum of the *Laque de Garance* paint sample. For comparison *Laque de Robert No.5* (yellow line) were added.

## FT-IR spectra

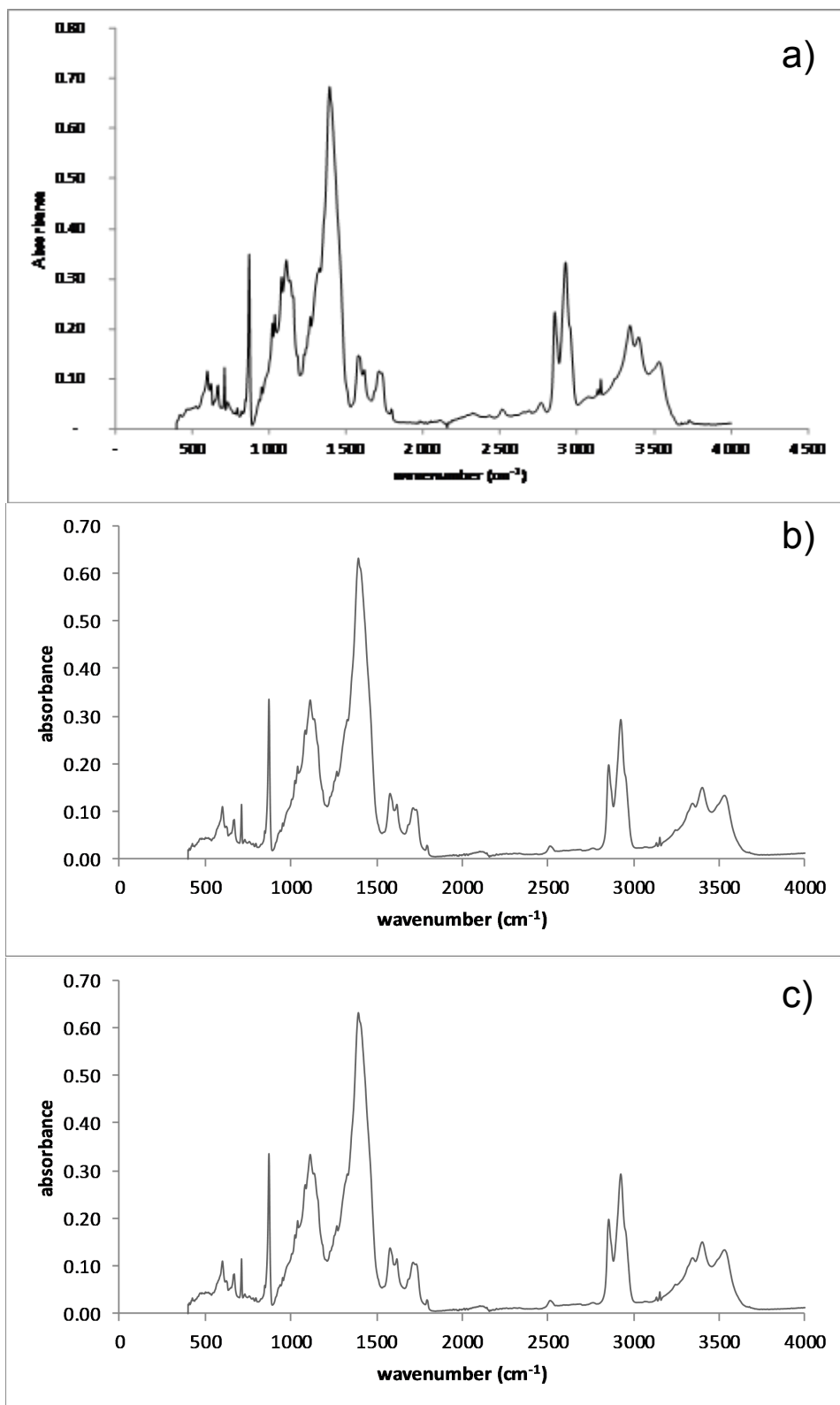


Fig. S43. FT-IR spectra of the: a) *Laque de Robert No. 5*, b) *Laque de Robert No. 6*, c) *Still de Grain* paint samples.